Efficient Unmanned Aerial Vehicles Assisted D2D Communication Networks

Wenson Chang[1(✉)], Kuang-Chieh Liu[2], Zhao-Ting Meng[3], and Li-Chun Wang[4]

[1] Department of Electrical Engineering, National Cheng-Kung University, Tainan, Taiwan R.O.C.
wenson@ee.ncku.edu.tw
[2] Realtek Semiconductor Co. Limited, Hsinchu, Taiwan R.O.C.
x3334226x@gmail.com
[3] SiliTai Electronics Co. Limited, Zhubei, Taiwan R.O.C.
fateric885522@gmail.com
[4] Department of Electrical Engineering, National Chiao-Tung Unversity, Hsinchu, Taiwan R.O.C.
lichun@faculty.nctu.edu.tw

Abstract. Nowadays, mounting a base-station (BS) onto an unmanned aerial vehicle (UAV) has become a new dimension for constructing the new generation of wireless communication networks. For example, dynamically constructing an UAV-BS network can provide some instantaneous and emergent communication services when the infrastructure of the cellular network is destroyed owing to some devastating disasters. In this paper, we aim to deploy a scalable and self-organized UAV-assisted device-to-device (D2D) communication network using a minimum number of UAV-BSs (UBSs) under some link quality constraints. Specifically, a sequential UBS deploying algorithm is designed to guarantee the signal quality for the links between the UBSs and ground terminals, and those between UBSs and central controller. Via the simulation results, it is interesting to find that how to deploy a proper number of UBSs rather than constructing a highly connected UBS network is the key to guarantee higher spectrum efficiency for the UBS-assisted D2D networks.

Keywords: UAV-assisted network · Fiedler value · D2D communications · 3D network · Laplacian matrix

This paper was jointly supported by Ministry of Science and Technology (under the Grant Numbers 108-2634-F-009-006, 109-2634-F-009-018 and 109-2221-E-006-176-MY2 through Pervasive Artificial Intelligence Research (PAIR) Lab and wireless communications and network Lab (WCNLAB), Taiwan) and QualComm Tech. INC. (under the Contract Numbers NAT-408931 and NAT-435536.).

H. Gao et al. (Eds.): ChinaCom 2020, LNICST 352, pp. 729–741, 2021.
https://doi.org/10.1007/978-3-030-67720-6_50

1 Introduction

Providing ubiquitous and high-quality communication services has always been the ultimate goal for the new generation of wireless communication systems. As the technology of unmanned aerial vehicle (UAV) becomes more and more mature, the UAV-assisted communications has emerged to be a new dimension of wireless communication networks. Generally speaking, mounting a base-station (UBS) on to a UAV (i.e., the namely UBS) can efficiently reconstruct the communication network when the infrastructure is devastated by large-scale disaster [1,2]. Also, it can be utilized to extend the coverage areas and collect data in some hazardous environments [3]. In some special events, the UBS can provide additional capacity and on-demand communication services [4,5]. More recently, incorporating UBSs into the framework of mobile edge computing further extends the frontier of high-speed and low-latency services [6,7].

In principle, the performance of an UAV-assisted network highly depends on two pivotal factors, i.e., the connectivity between UAVs [8–11] and its deployment scheme, including the flying trajectory arrangement [12–19]. In the aspect of interconnectivity between UAVs, the authors in [8] used the second eigenvalue of the Laplacian matrix (i.e., so-called Fiedler value [20]) to evaluate the connectivity of the UBS network. And thus, the main principle of deploying an UBS is to guarantee the signal-to-noise power ratio (SNR) requirements for the mobile terminals (MTs) on the ground, while achieving the highest Fiedler value for the whole network. In [9], a centralized algorithm was proposed to deploy a proper number of UBSs to serve a given number of MTs under the constraint of the inter-connectivity of UBSs. However, the methods of overall deployment and then one-by-one eliminating the unnecessary connections for MTs and idle UBSs based on the so-called degrees (i.e., the connection opportunities for each MT and UBS, respectively) cannot guarantee the minimum number of UBSs and the maximum connectivity between UBSs. In [10], the UAVs were deployed as the relays to reconstruct the post-disaster communication network. Specifically, three phases were designed to select the optimal positions, including the network traversing, coverage hole detection and deployment phases, so that the damaged network can be recovered autonomously. In [11], the interconnected UAVs were used to facilitate the data delivery for the intelligent transportation systems. Generally, the UAVs can develop the connections for the sparsely connected network on the ground. Then, with aid of UAVs, the routing path which avoids obstructions at the cost the limited overheads can be constructed and maintained.

In the aspect of UAV deployment, the reverse neural network model was applied in [17] to properly deploy UAVs such that the network coverage and overall throughput can be improved. In [12], the UAV-assisted three-hop transmission scheme was designed to deliver packets between two fixed sites on the ground. Therein, the optimal UAV trajectory was designed by taking several constraints into account (including the constraints of the transmit power, UAV mobility, collision avoidance and information causality) so that the end-to-end throughput can be maximized. To solve the non-convex problem, the so-called alternating

maximization and successive convex optimization techniques were applied to develop an iterative trajectory algorithm. In [13], multiple solar-powered UBSs were deployed to improve the energy-efficiency of the heterogeneous network on the ground. To achieve this, an linear programming problem was formulated by taking the constraints of quality-of-service (QoS) and cells' capacity into consideration. With aid of UBSs, the small-cells on the ground can be switched into the sleep mode so as to minimize the energy consumption. In [14], to maximize the QoS for users while guaranteeing the backhaul connections, the probability density function of users' locations was taken into account when deciding the locations of UBSs. In [16], the multiple UBSs were sequentially deployed according to a incycloduction-spiral path until all the ground users can access more than one UBSs. In this way, the unnecessary UBS deployments can be eliminated. In [18], the coexistence of UAV-assisted and device-to-device (D2D) networks were considered for two cases: (1) analytically deciding the optimal altitude of the fixed UAVs according to the density of D2D users such that maximal coverage of UAV-assisted network can be achieved; and (2) analytically deciding the minimum stop points of mobile UAVs to reach a better tradeoff between the delay and coverage of UAV-assisted network, and the outage probability of D2D network. In [19], the backhaul connections between the UAVs and gateway were developed by deploying the multi-hop UAV-assisted networks. Under this scenario, the non-convex optimization problem was formulated to maximize the downlink throughput subject to the constraints of flow conservation. Then, using the mentioned alternating maximization and successive convex optimization techniques were applied to decide the locations of UAVs, and the allocations of bandwidth and transmission power, respectively.

According to the above discussions, we found that jointly consider the interconnectivity between UBSs, and that between UBSs and backhual links under the QoS constraints for all the links (including links between the UBSs and the ground users) was neglected from the literature. Thus, in this paper, we aim to develop a scalable and self-organized UBSs network to facilitate the D2D communications under the QoS constraints for all the links. To accomplish this goal, the minimal number of UBSs are sequentially deployed to serve the ground users under the mentioned constraints for all the links; and at the meantime, the interconnectivity between UBSs can be guaranteed. According to the simulation results, we find that how to deploy a proper number of UBSs rather than constructing a highly connected UBS network is the key to guarantee higher spectrum efficiency for the UBS-assisted D2D networks.

The rest of this paper is organized as follows. In Sect. 2, the system model, including the signal model and definition of the interconnectivity between UBSs are introduced. In Sect. 3, the optimization problem of UBS deployment will be formulated and solved by proposing a sequential UBS deployment algorithm. At last, Sects. 4 and 5 render the simulation results and concluding remarks, respectively.

2 System Model

Consider that a set of UAV-BS (denoted by $\boldsymbol{\Omega} = \{\Omega_i\}\ \forall i = 1, \cdots, N$) are deployed to serve M groups of mobile terminal (denoted by $\mathbf{M} = \{\mathbf{m}_j\}\ \forall j = 1, \cdots, M$); and each group consists of $|\mathbf{m}_j|$ MTs (denoted by $\mathbf{m}_j = \{m_{jk}\}\ \forall k = 1, \cdots, |\mathbf{m}_j|$), where $|\mathbf{m}_j|$ calculates the number of elements in the set $\mathbf{m}_j$. Moreover, a UBS controller (denoted by Ω_o) is deployed to govern all the activities of UBSs, including the collections and exchanges for all the data and control information. Figure 1 demonstrates a sketch for the considered system scenario, where $N = 3$ UBSs are deployed to serve $M = 5$ groups of MTs; and within each group there are $|\mathbf{m}_j| = 5\ \forall j = 1, \cdots, M$ MTs.

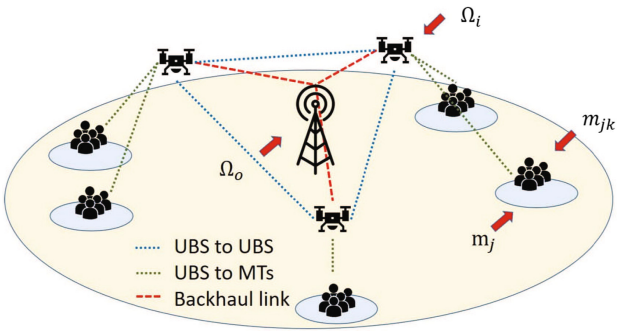

Fig. 1. System model

2.1 Signal Model

To begin with, the orthogonal channels are allocated to all the links between (1) two arbitrary neighboring UBSs, (2) UBS and MT and (3) UBS and controller Ω_o [8,13]. Also, according to [8,9,13,18], the impact of small-scale fading is generally neglected for the air-to-air and air-to-ground channel environments; and that, solely the effect of the path-loss is considered to characterize these two environments. Therefore, with LoS channel, the signal-to-noise power ratio (SNR) for the link between Ω_i and Ω_j (denoted by $\mathcal{L}_{ij}$) can be defined as

$$\gamma_{ij} = \frac{P_\Omega d_{ij}^{-\alpha}}{\sigma^2}\ , \tag{1}$$

where d_{ij} denotes the length of the link $\mathcal{L}_{ij}$ (i.e., the geographical distance between Ω_i and Ω_j); α and P_Ω stand for the path-loss exponent and transmission power of UAV, respectively; σ^2 represent the variance of the zero-meaned additive white Gaussian noise (AWGN). However, in addition to the LoS channel environment, it is highly possible to have non-LoS (NLoS) channel between UBSs and ground terminals, e.g., the MT or the controller Ω_o, respectively.

Thus, referring to [13], the path-loss for the air-to-ground link between Ω_i and m_{jk} (denoted by $\mathcal{L}_{ijk}$) can be defined as

$$g_{ijk}^{\varphi} = 20\log_{10}\left(\frac{4\pi\hat{d}_{ijk}}{\lambda_0}\right) + \xi_{\varphi}\ (\text{dB}), \tag{2}$$

where $\hat{d}_{ijk}$ denotes the length of $\mathcal{L}_{ijk}$; λ_o represent the wave-length corresponding to the carrier frequency; $\varphi \in \{\text{LoS, NLoS}\}$ indicates the LoS and NLoS cases, respectively. By analogy, the path-loss g_{io}^{φ} between Ω_i and Ω_o (i.e., the link $\mathcal{L}_{io}$) can also be defined by substituting the length of $\mathcal{L}_{io}$ (say d_{io}) into (2).

To characterize the random effect of LoS and NLoS channel for the air-to-ground link, the LoS probability for the link $\mathcal{L}_{ijk}$ (denoted by $P_{LoS}(\mathcal{L}_{ijk})$) can be defined as

$$P_{LoS}(\mathcal{L}_{ijk}) = \left(\frac{1}{1+\nu_1\exp\left(-\nu_2\left[\theta_{ijk}-\nu_1\right]\right)}\right)\ , \tag{3}$$

where ν_1 and ν_2 reflect the environmental effects; θ_{ijk} denotes the elevation angle between Ω_i and m_{jk}. By definition, the NLoS probability can be defined as $P_{NLoS} = 1 - P_{LoS}$. Note that the LoS probability for the link $\mathcal{L}_{io}$ can also be defined by replacing θ_{ijk} of (3) with θ_{io} (i.e., the elevation angle between Ω_i and Ω_o). Then, the average path-loss for the link $\mathcal{L}_{ijk}$ can be calculated as

$$\bar{g}_{ijk} = \sum_{\varphi\in\{\text{LoS, NLoS}\}} P_{\varphi}(\mathcal{L}_{ijk}) g_{ijk}^{\varphi}\ . \tag{4}$$

Similarly, the average path-loss $\bar{g}_{io}$ for the link $\mathcal{L}_{io}$ can also be defined by replacing $\mathcal{L}_{ijk}$ of (4) with $\mathcal{L}_{io}$. At last, the SNR for the links $\mathcal{L}_{ijk}$ and $\mathcal{L}_{io}$ (denoted by γ_{ijk} and γ_{io}) can be obtained by substituting $\bar{g}_{ijk}$ and $\bar{g}_{io}$ into $d_{ij}^{-\alpha}$ of (1), respectively.

2.2 Connectivity of UBS Network

To well describe connectivity of the UBS network, a graph $\mathcal{G}(\mathcal{V},\mathcal{E})$ can be constructed by using each UBS as each vertex; and an edge can then be constructed if the corresponding two UBSs (i.e., two vertices in other words) are reachable to each other (i.e., the distance in-between should be less than the serving distance d_{Ω}), where $\mathcal{V}$ and $\mathcal{E}$ denote the set of vertices and connected edges, respectively. To facilitate the presentation, let $V_i \in \{\mathcal{V}\}$ denote the vertex corresponding to Ω_i; and similarly, the edge $E_{ij}^{(\ell)} \in \{\mathcal{E}\}$ stands for the ℓ-th edge in $\mathcal{E}$ connecting V_i and V_j. Moreover, let's define edge vector $\mathbf{a}_\ell = [a_{\ell,i}]^T$ corresponding to $E_{ij}^{(\ell)}$ $\forall a_{\ell,i} \in \{0,1\}\,,\ i = 1,\cdots,|\mathcal{V}|,\ \ell = 1,\cdots,|\mathcal{E}|$, where $|\mathcal{V}|$ and $|\mathcal{E}|$ calculates the number of elements in the set $\mathcal{V}$ and $\mathcal{E}$, respectively. Then, with $E_{ij}^{(\ell)}$, it results in $a_{\ell,i} = a_{\ell,j} = 1$, which means V_i is in the coverage area $\mathcal{A}_j$ of V_j (denoted by $V_i \in \mathcal{A}_j$) and vice versa (denoted $V_j \in \mathcal{A}_i$). Note that each edge vector can only have two non-zero elements for describing its corresponding edge.

Then, the Laplacian matrix $\mathbf{L}$ can be defined as

$$\mathbf{L} = \mathbf{A}\text{diag}(\mathbf{w})\mathbf{A}^T = \sum_{\ell=1}^{|\mathcal{E}|} w_\ell \mathbf{a}_\ell \mathbf{a}_\ell^T \ , \tag{5}$$

where the matrix $\mathbf{A}$ is constructed by using the edge vectors; diag($\mathbf{w}$) is the diagonal matrix constructed by using the weight vector $\mathbf{w} = \{w_\ell\}\ \forall \ell = 1, \cdots, |\mathcal{E}|$ [8,20]. Note that according to (5), one can know that $\mathbf{L}$ is semi-positive definite, which means all the corresponding eigenvalues are non-negative. In fact, its first smallest eigenvalue is zero; and the second smallest one (denoted by $\lambda_2(\mathbf{L})$) is defined as the so-called Fielder value. According to the graph theory, the Fielder value can be used to characterize the connectivity of the network. By definition, the larger the Fielder value, the better the connectivity of the network. As $\lambda_2(\mathbf{L}) = 0$, it is said that the network is completely disconnected. It should be noticed that as the connectivity increases, more edges can be constructed. That means there will be more edge vectors and consequently the size of the Laplacian matrix $\mathbf{A}$ increases (e.g., more UBSs are hovering in the air).

3 Problem Formulation and UBS Deployment Scheme

In this paper, we aim to develop an efficient UBS-assisted D2D network by deploying the minimum number of UBSs. To this end, the positions of the hovering UBSs (denoted by $\mathbf{U} = \{(x_i, y_i, z_i)\}\ \forall \Omega_i \in \boldsymbol{\Omega}$) should be properly decided such that the considered groups of MTs on the ground can be well-severed, where (x_i, y_i, z_i) means the coordination of the Ω_i within the three-dimensional space. To clarity, the term "well-served" means two conditions are satisfied: (1) the SNR constraints for all the MTs belonging to the considered MT groups, and (2) the SNR constraints for the link between Ω_i and Ω_o. Moreover, the connectivity of the UBS network should be maintained as well. In this fashion, the self-organized D2D network can be developed. Then, the optimization problem of interest can be formulated as

$$\begin{aligned} \max_{\mathbf{U}} \min_{\boldsymbol{\Omega}} \ & \lambda_2(\mathbf{L}(\mathbf{U})) \\ \text{s. t. } & \gamma_{ijk} \geq \gamma_{th} \ \forall \ \Omega_i \in \boldsymbol{\Omega} \ , \ m_{jk} \in \mathbf{m}_j \in \mathbf{M} \\ & \gamma_{io} \geq \gamma_{th} \ \ \forall \ \Omega_i \in \boldsymbol{\Omega} \ . \end{aligned} \tag{6}$$

where γ_{th} is the SNR threshold. It should be noticed that to well maintain the connectivity between UBSs, the weight w_ℓ for $E_{ij}^{(\ell)}$ is designed to be $d_{ij}^{-\alpha}$.

Prior to developing the UBS deployment algorithm, several terminologies are defined as follows.

1. $\mathcal{A}_{oj}$: the square area formed by using Ω_o and the center of $\mathbf{m}_j$ as the two vertices on the diagonal.
2. $\mathcal{A}_{ij}$: the areas in which the UBS Ω_i can well-serve the MT groups $\mathbf{m}_j$.
3. $\boldsymbol{\Phi}_i$: the set of MT groups which can be well-served by the UBS Ω_i.

4. $\Pi_{\mathbf{m}_j \in \boldsymbol{\Phi}_i} \mathcal{A}_{ij}$: the intersected area in which the UBS Ω_i can well-serve the MT group $\mathbf{m}_j \in \boldsymbol{\Phi}_i$.
5. d_{jn}: the distance between the centers of the MT groups $\mathbf{m}_j$ and $\mathbf{m}_n$.
6. d_{jo}: the distance between the centers of the MT groups $\mathbf{m}_j$ and Ω_o.

Moreover, two conditions are make: (1) all the UBSs are at the same height h_Ω m (i.e., $z_i = h_\Omega \, \forall \Omega_i \in \boldsymbol{\Omega}$); and (2) the coordinate plane at $z_i = h_\Omega$ is discretized with space granularity μ point/m^2.

Now, to solve (6), we develop the sequential UBS deployment scheme as listed in Algorithm 1. Observing Algorithm 1, one can find that Lines 6 and 10 dominate the computational complexity. Specifically, the two while-loops on Lines 4 and 9 requires computations of order $\mathcal{O}(M^2)$; whereas searching for the "well-served areas" on Lines 6 and 10 maximally needs to scanning $\mathcal{A}_{oj} \times \mu$ points over the mentioned coordinate plane. To sum up, Algorithm 1 needs computations of order $\mathcal{O}(M^2 \times \mathcal{A}_{oj} \times \mu)$, which mainly depends on the granularity (i.e., μ) and distribution of the MT groups (i.e., $\mathcal{A}_{oi}$ in other words), respectively.

It should be noticed that Line 3 guarantees the maximal area of $\mathcal{A}_{oi}$ for the searching processes on Lines 6 and 10. Accordingly, it gives the most opportunities for Lines 10–12 to serve the most MT groups; and for Line 15 to maximize the Fiedler value $\lambda_2(\mathbf{L}(\mathbf{U}))$. This somehow verifies the optimality of the proposed UBS deploy algorithm with the prescribed order of complexity. Moreover, the proposed algorithm can be scalable by interatively treating each UBS as a new controller to the further deploy some additional UBSs for extending the overall coverage area. That means these additional UBSs can keep connected to the original central controller via some multi-hop (rather than one-hop) transmission path.

4 Simulation Result

In this section, we verify the effectiveness of the proposed sequential UBS deployment algorithm by comparing with the counterpart in [8] in terms of the number of hops, SE and Fiedler value. Note that in [8], each UBS is deployed for serving each MT group under the condition of maximizing the Fiedler value; whereas, in the proposed scheme, a UBS can possibly serve multiple MT groups. For fair performance comparison, the simulation environment is built by referring to that in [8]. In addition, to make it more practical, the scale of the 3D network is expanded to cover a square area of 1000×1000 m^2. Also, the back haul connection to the UBS controller is newly included (i.e., the constraint of γ_{io} in (6)). Moreover, the effects of the LoS and NLoS channel environment in [13] is considered as well. Table 1 summarizes all the simulation parameters; and all the results are obtained by averaging over 1,000 randomly generated network topologies.

4.1 Number of Hops

Figure 2 shows the impact of the SNR requirement γ_{th} on the number of hops for the UAV-assisted D2D communication networks, where (a) $\gamma_{th} = 40$ dB, (b)

Algorithm 1: Sequential UBS Deployment Algorithm

Input: $\mathbf{M}$;
Output: $\boldsymbol{\Omega}$, $\mathbf{U}$;

Let $\boldsymbol{\Omega} = \mathbf{U} = \hat{\mathbf{M}} = \emptyset$;
$i = 1$;
Sort all the MT groups $\mathbf{m}_\ell$ $\forall \ell = 1, \cdots, M$ according to $\check{d}_{\ell o}$; and restore the results back to $\mathbf{M}$ in the descending order;
while $\mathbf{M} \neq \emptyset$ **do**
    Consider the first MT group from the top of $\mathbf{M}$ and let it be $\mathbf{m}_j$;
    Find $\mathcal{A}_{ij}$ within $\mathcal{A}_{oj}$;
    Sort all the MT groups $\mathbf{m}_n \in \mathbf{M}$ $\forall n \neq j$ according to the distance $\check{d}_{jn}$ to $\mathbf{m}_j$ in the ascending order and store the results into $\hat{\mathbf{M}}$;
    $\boldsymbol{\Phi}_i = \mathbf{m}_j$; $k = 1$;
    while $\hat{\mathbf{M}} \neq \emptyset$ **do**
        Find $\mathcal{A}_{ik}$ within $\mathcal{A}_{ij}$ for $\mathbf{m}_k \in \hat{\mathbf{M}}$;
        if $\mathit{\Pi}_{\mathbf{m}_n \in (\boldsymbol{\Phi}_i \cup \mathbf{m}_k)} \mathcal{A}_{in} \neq \emptyset$ **then**
            $\boldsymbol{\Phi}_i = \boldsymbol{\Phi}_i \cup \mathbf{m}_k$;
        $\hat{\mathbf{M}} = \hat{\mathbf{M}} \setminus \mathbf{m}_k$;
        $k = k + 1$;
    Search for a point (x_i, y_i, z_i) nearest to Ω_o within $\mathit{\Pi}_{\mathbf{m}_n \in \boldsymbol{\Phi}_i} \mathcal{A}_{in}$ so that $\lambda_2(\mathbf{L}(\mathbf{U}))$ can be maximized;
    $\boldsymbol{\Omega} = \boldsymbol{\Omega} \cup \Omega_i$;
    $\mathbf{U} = \mathbf{U} \cup (x_i, y_i, z_i)$;
    $\mathbf{M} = \mathbf{M} \setminus \boldsymbol{\Phi}_i$;
    $i = i + 1$;
Return $\{\boldsymbol{\Omega}, \mathbf{U}\}$;

$\gamma_{th} = 45\,\text{dB}$ and (c) $\gamma_{th} = 50\,\text{dB}$, respectively. In the simulations, the transmitting and receiving ends of a D2D pair are randomly deployed into two different MT groups, respectively. Observing these figures, one can apparently find that the number of hops increases as γ_{th} grows. There are two reasons for this phenomenons. Firstly, with higher requirements of link quality (i.e., γ_{th} in other words), the UBSs tend to hovering in the air near their served MT groups; and consequently, the distance between two arbitrary UBSs increases. Therefore, the connectivity of the UBS network reduces; and more hops are needed to develop a routing path for a D2D pair. Secondly, for the proposed scheme, more UBSs should be deployed to provide links with higher quality (as demonstrated in the following Fig. 3), which results in more required hops as well. Furthermore, in either cases of γ_{th}, less hops are required to develop the routing paths for the D2D network using the proposed scheme. For the example with $\gamma_{th} = 40\,\text{dB}$, approximately one hop can be saved for 80% of the D2D transmissions.

Table 1. Simulation parameters

Parameter	Value
Operational mode of UBS	Half-duplex transmissions
Average additional loss ξ_{LoS}	1 dB [13]
Average additional loss ξ_{NLoS}	12 dB [13]
Environment effects ν_1 and ν_2	9.6 and 0.29 [13]
Wavelength λ_0	0.125 m [13]
Path loss exponent α	2 [8]
The transmission power of UAV P_Ω	0.1 W [8]
Variance of AWGN σ^2	-174 dBm/HZ
System bandwidth	1 MHz
UAV height h_Ω	40 m
Area of network topology	$1000 \times 1000\,\mathrm{m}^2$
Number of MT groups M	5
Number of MT in each group $\lvert\mathbf{m}_j\rvert$	$5\ \forall j = 1, \cdots, 5$
Radius of MT group	20 m
Serving distance of UBS d_Ω	100 m
Space granularity μ	$1\ 1/\mathrm{m}^2$

4.2 Spectrum Efficiency and Fiedler Value

Figure 3 shows the impact of the SNR requirement γ_{th} on the (a) 10-percentile SE (denoted by $SE_{10\%}$) and (b) Fiedler value for the UAV-assisted D2D communication networks, respectively. Herein, the so-called 10-percentile SE is obtained by properly taking an threshold for the probability cumulative distribution function of SE (i.e., the *cdf* curve of SE) so that 90% of the SE can be higher than γ_{th}. As explained in Fig. 2, a higher γ_{th} can lead to longer distance between any two arbitrary UBSs, which lowering the connectivity of the UBS network. Moreover, as the γ_{th} keeps increasing, more UBSs are required when the proposed scheme is applied; and consequently the Fielder value can rise. However, the higher Fiedler values don't always means the higher SE. De facto, it is interesting to find that the UBS network with lowest Fiedler value (i.e., the loosely connected UBS network in other words) can achieve the highest $SE_{10\%}$. This phenomenon is somehow contradicted to the general intuition and the goal of [8,20]. Therefore, one can say that how to deploy a proper number of UBSs rather than constructing a UBS network with higher Fielder value is the key to guarantee a higher SE for the UBS-assisted D2D networks.

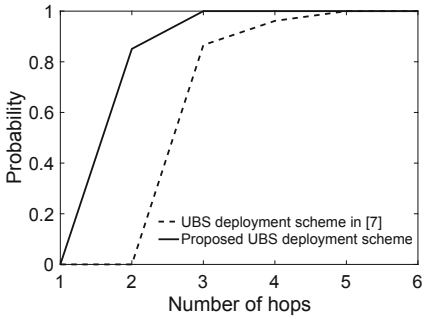

(a) $\gamma_{th} = 40$ dB

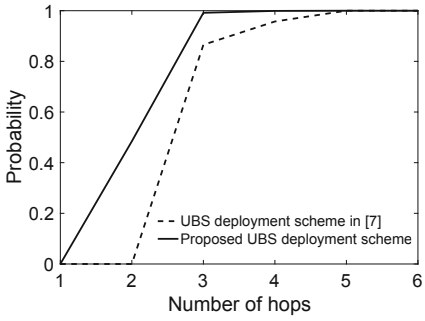

(b) $\gamma_{th} = 45$ dB

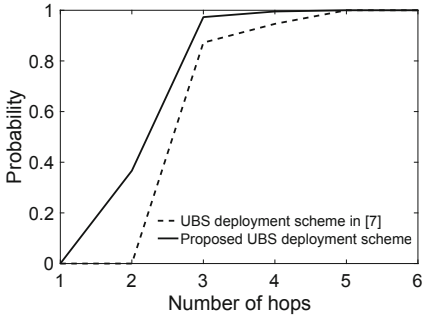

(c) $\gamma_{th} = 50$ dB

Fig. 2. Impact of the SNR requirement γ_{th} on the number of hops for the UAV-assisted D2D communication networks, where (a) $\gamma_{th} = 40\,\mathrm{dB}$, (b) $\gamma_{th} = 45\,\mathrm{dB}$ and (c) $\gamma_{th} = 50\,\mathrm{dB}$, respectively.

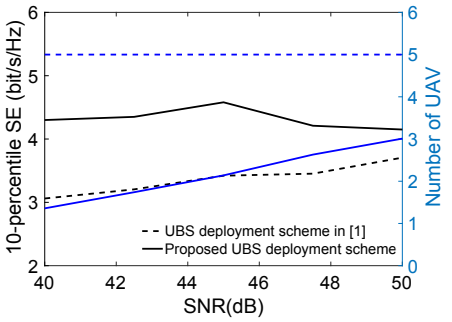

(a) 10-percentile SE (bps/Hz)

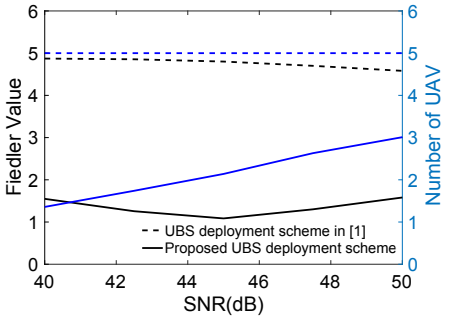

(b) Fiedler value

Fig. 3. Impact of the SNR requirement γ_{th} on the (a) 10-percentile SE (denoted by $SE_{10\%}$) and (b) Fiedler value for the UAV-assisted D2D communication networks, respectively.

5 Conclusions and Future Works

In this paper, we have developed a scalable UBS deployment algorithm to construct an UAV-assisted D2D communication network. Using the proposed algorithm, a self-organized 3D network can be constructed to provide some instantaneous and emergent communication services, especially for the cases when the infrastructure of cellular network become malfunctioned. Specifically, to guarantee the reliability and efficiency, a minimum number of UBSs are properly deployed under the SNR constraints for links between UBSs and ground terminals. Moreover, the links between the UBSs and center controller are included, as well. The efficiency of the self-organized 3D network has been verified by simulations in terms of the number of hops and spectrum efficiency, respectively. Most importantly, an counterintuitive phenomenon has been observed that a highly connected UBS network cannot always guarantee a higher spectrum efficiency. Instead, how to deploy a proper number of UBSs is key for constructing a high efficient UBS-assisted D2D network. It is well-known that steadily hovering in the air for a long period of time is fatal to the success of the UBS-assisted

communication network. One important factor behind is the energy-efficiency (EE) of the UBS, including its energy-harvest (ER) capability. Therefore, incorporating the EE as well as the ER method into the proposed scheme can be an important topic for further study.

References

1. Zhao, N., et al.: UAV-assisted emergency networks in disasters. IEEE Wirel. Commun. **26**(1), 45–51 (2019)
2. Erdelj, M., Natalizio, E., Chowdhury, K.R., Akyildiz, I.F.: Help from the sky: leveraging UAVs for disaster management. IEEE Perv. Comput. **16**(1), 24–32 (2017)
3. Tazibt, C.Y., Achir, N., Muhlethaler, P., Djamah, T.: UAV-based data gathering using an artificial potential fields approach. In: IEEE Vehicular Technology Conference (VTC-Fall), pp. 27–30, August 2018
4. Li, Y., Cai, L.: UAV-assisted dynamic coverage in a heterogeneous cellular system. IEEE Netw. **31**(4), 56–61 (2017)
5. Wang, X., Feng, W., Chen, Y., Ge, N.: Sum rate maximization for mobile UAV-aided internet of things communications system. In: IEEE 88th Vehicular Technology Conference (VTC-Fall), pp. 27–30, August 2018
6. Zhou, F., Wu, Y., Hu, R.Q., Qian, Y.: Computation rate maximization in UAV-enabled wireless-powered mobile-edge computing systems. IEEE J. Sel. Areas Commun. **36**(9), 1927–1941 (2018)
7. Zhang, X., Zhong, Y., Liu, P., Zhou, F., Wang, Y.: Resource allocation for a UAV-enabled mobile-edge computing system computation efficiency maximization. IEEE Access **7**, 113 345–113 354 (2019)
8. Abdel-Malek, M.A., Ibrahim, A.S., Di, X., Mokhtar, M.: Optimum UAV positioning for better coverage-connectivity tradeoff. In: IEEE Annual International Symposium on Personal, Indoor, and Mobile Radio Communications (PIMRC), pp. 1–5, September 2017
9. Zhao, H., Wang, H., Wu, W., Wei, J.: Deployment algorithms for UAV airborne networks toward on-demand coverage. IEEE J. Sel. Areas Commun. **36**(9), 2015–2031 (2018)
10. Park, S.-Y., Shin, C.S., Jeong, D., Lee, H.: DronenetX: network reconstruction through connectivity probing and relay deployment by multiple UAVs in ad hoc networks. IEEE Trans. Veh. Technol. **67**(11), 11 192–11 207 (2018)
11. Oubbati, O.S., Chaib, N., Lakas, A., Lorenz, P., Rachedi, A.: UAV-assisted supporting services connectivity in urban VANETs. IEEE Tran. Veh. Technol. **68**(4), 3944–3951 (2019)
12. Zhang, G., Yan, H., Zenga, Y., Cui, M., Liu, Y.: Trajectory optimization and power allocation for multi-hop UAV relaying communications. IEEE Access **6**, 48 566–48 576 (2018)
13. Alsharoa, A., Ghazzai, H., Kadri, A., Kamal, A.E.: Energy management in cellular hetnets assisted by solar powered drone small cells. In: IEEE Wireless Communications and Networking Conference (WCNC), pp. 1–6, March 2017
14. Savkin, A.V., Huang, H.: Deployment of unmanned aerial vehicle base stations for optimal quality of coverage. IEEE Wirel. Commun. Lett. **8**(1), 321–324 (2019)
15. Lagum, F., Bor-Yaliniz, I., Yanikomeroglu, H.: Strategic densification with UAV-BSs in cellular networks. IEEE Wirel. Commun. Lett. **7**(3), 384–387 (2018)

16. Lyu, J., Zeng, Y., Zhang, R., Lim, T.J.: Placement optimization of UAV-mounted mobile base stations. IEEE Commun. Lett. **21**(3), 604–607 (2017)
17. Sharma, V., Bennis, M., Kumar, Y.: UAV-assisted heterogeneous networks for capacity enhancement, pp. 1207–1210, June 2016
18. Mozaffari, M., Saad, W., Bennis, M., Debbah, M.: Unmanned aerial vehicle with underlaid device-to-device communications: performance and tradeoffs. IEEE Trans. Wireless Commun. **15**(6), 3949–3963 (2016)
19. Li, P., Xu, J.: UAV-enabled cellular networks with multi-hop backhauls: placement optimization and wireless resource allocation. In: IEEE International Conference on Communication Systems (ICCS), pp. 110–114, December 2018
20. Ibrahim, A.S., Seddik, K.G., Liu, K.J.R.: Connectivity-aware network maintenance and repair via relays deployment. IEEE Trans. Wireless Commun. **8**(1), 356–366 (2009)